

DIRECT MAPPING OF MASSIVE COMPACT OBJECTS IN EXTRAGALACTIC DARK HALOS

KAIKI TARO INOUE AND MASASHI CHIBA

Division of Theoretical Astrophysics, National Astronomical Observatory, 2-21-1 Osawa, Mitaka, Tokyo 181-8588, Japan;

tinoue@th.nao.ac.jp, chibams@gala.mtk.nao.ac.jp

NAOJ-Th-Ap2003, No.22

ABSTRACT

A significant fraction of non-baryonic or baryonic dark matter in galactic halos may consist of MASSive Compact Objects (MASCOs) with mass $M = 10^{1-4}M_{\odot}$. Possible candidates for such compact objects include primordial black holes or remnants of primordial (Population III) stars. We propose a method for directly detecting MASCOs in extragalactic halos, using the VLBI techniques with extremely high resolution that would be achieved by the next generation mission of the VLBI Space Observatory Program such as VSOP-2. If a galactic halo comprising a large number of MASCOs produces multiple images of a background radio-loud QSO by gravitational lensing, then a high-resolution radio map of each macro-lensed image should reveal microlensing effects by MASCOs. To assess their observational feasibility, we simulate microlensing of the radio-loud, four-image lensed QSO, B1422+231, assuming angular resolution of ~ 0.01 mas. MASCOs are represented by point masses. For comparison, we also simulate microlensing of B1422+231 by singular isothermal spheres. We find that the surface brightness of the macro-lensed images shows distinct spatial patterns on the scale of the Einstein radius of the perturbers. In the case of point-mass perturbers, many tiny dark spots also appear in the macro-lensed images associated with a decrease in the surface brightness toward the fringe of the original QSO image, whereas no such spots are available in the SIS models. Because such spatial patterns in each macro-lensed image cannot be linearly mapped to those in other macro-lensed images if they are relevant to lensing perturbers, it is fairly easy to discriminate them from intrinsic substructures within a QSO. Based on the size, position and magnified or demagnified patterns of images, we shall be able to determine the mass and density profile of an individual MASCO as well as its spatial distribution and abundance in a galactic halo.

Subject headings: gravitational lensing – dark matter – galaxies: cluster – stars: Population III

1. INTRODUCTION

Gravitational lensing is a powerful tool for probing dark matter in the form of compact objects, such as black holes, neutron stars, and dwarfs. To date, various kinds of gravitational lensing studies give stringent upper limits on the abundance of these objects on very different mass scales, ranging from sub-stellar objects $\sim 10^{-7}M_{\odot}$ (Alcock et al. 2000) to galaxy clusters $\sim 10^{14}M_{\odot}$ (Nemiroff 1991).

However, there have been no stringent observational constraints on dark compact objects with a mass range of $10^1M_{\odot} \lesssim M \lesssim 10^4M_{\odot}$ corresponding to the mass range of massive stars. For brevity, we call them MASCOs (MASSive Compact Objects). It is of particular importance to constrain their abundance in galactic dark halos, because MASCOs are both baryonic and non-baryonic dark matter candidates. Recent observation of the cosmic microwave background (Bennett et al. 2003) suggests that the primordial stars (or Population III stars) are rather massive as indicated by theoretical works (Bromm, Coppi, & Larson 1999; Abel, Bryan, & Norman 2000; Tsuribe & Inutsuka 2001; Omukai & Palla 2002) and their formation efficiency are higher than current theoretical works suggest (Cen 2003). In some MASCO mass scales, primordial stars collapse directly to form black holes (Bond et al. 1984; Woosley 1986). Thus, a large fraction of baryonic dark matter in galactic dark halos may consist of black holes that are remnants of massive primordial stars. Alternatively, as the cold dark matter (CDM) candidates, MASCOs may be primordial black holes that are produced in the early universe at the era between the QCD phase transition and the big-bang nucleosynthesis (Carr 1975).

To date, various gravitational lensing methods that can probe MASCOs have been proposed. Gould (1992) proposed that an-

nual oscillation in the light curve of a MACHO lensing event can distinguish a MASCO from a stellar mass compact object. However, for a mass range of $10^2M_{\odot} \lesssim M \lesssim 10^3M_{\odot}$, the annual oscillation owing to the Earth's motion is too small to determine the transverse velocity. Totani (2003) argued that observation of cluster-cluster microlensing system by a 8 m-class ground-based telescope can probe the abundance of compact objects with mass $10^{-5}M_{\odot} \lesssim M \lesssim 10^{12}M_{\odot}$. Although his proposed method covers a wide range of mass scales, the method itself cannot break the degeneracy in the lensing parameters such as mass or transverse velocity owing to the lack of information of the source star luminosity.

As an alternative, we propose a method to directly detect MASCOs using the VLBI techniques with extremely high resolution. Suppose that a distant radio-loud QSO shows multiple images owing to the lensing effect of a foreground galaxy. If there are a large number of MASCOs in the galactic halo, then the high-resolution radio map of the gravitationally lensed QSO images should reveal the microlensing effects by MASCOs. In contrast to the previous methods, our proposed method can determine the mass of MASCOs in the dark halo without any assumption on the lensing parameters. Furthermore, we can also prove the spatial distribution of MASCOs in the dark halo projected onto the surface perpendicular to the line of sight. A possible target lens system is B1422+231 in which the source is a radio-loud QSO at redshift $z_s = 3.62$ and the lens is an elliptical galaxy at redshift $z_L = 0.34$. Although the method we propose here is similar to that of Wambsganss & Paczyński (1992) in which the target compact object mass is set to $M \sim 10^6M_{\odot}$, the lensing effect by MASCOs can be quite different since the Einstein radius is much smaller than the size of a source and the

total number in a dark halo is large. In this *Letter*, we show our simulation results for the lens system B1422+231 microlensed by MASCOs, that would be observable by the future VLBI network.

We propose to construct a new VLBI network with extremely high resolution such as the planned next generation VLBI Space Observatory Program (VSOP-2) (Hirabayashi et al. 2001) and produce high resolution maps of strongly lensed radio-loud QSOs such as B1422+231. Such maps might provide us with valuable information of the first star remnants and the initial condition of density fluctuations on MASCO scales as well as the nature of the CDM.

2. METHOD

We consider a lensing system in which a radio-loud QSO is strongly lensed by the dark halo of an intervening galaxy. If MASCOs constitute a large amount of the dark matter component, then we expect to see many microlensing events by them, because the microlensing optical depth is nearly 1 in a strong lens. In order to detect the signatures of such microlensing in the macro-lensed QSO images, one needs extremely high-resolution radio mapping of the images. The necessary resolution can be estimated by the Einstein radius of MASCOs

$$\theta_E \sim 3 \times 10^{-2} \left(\frac{M}{10^2 M_\odot} \right)^{\frac{1}{2}} \left(\frac{D_L D_S / D_{LS}}{\text{Gpc}} \right)^{-\frac{1}{2}} \text{ mas}, \quad (1)$$

where D_L , D_S , and D_{LS} are the angular diameter distance to the lens, source, and distance to the lens from the source, respectively. Although current observations cannot achieve such a high-resolution, it is not out of reach in the near future. For instance, the target resolution of the VSOP-2 mission is ~ 0.025 mas at 43 GHz, which can resolve MASCOs with mass $M \gtrsim 10^2 M_\odot$ for lensing systems at 1 Gpc. The VSOP-2 satellite will be placed at an elliptical orbit with an apogee height of $\sim 30,000$ km and a perigee height of $\sim 1,000$ km (Hirabayashi et al. 2001). The resolution can be further improved by a factor of two or three by placing satellite(s) at a much distant orbit or by increasing the observational frequency.

In order to demonstrate the microlensing effects of MASCOs, we consider the QSO lensing system B1422+231 whose images consist of three highly magnified ones A, B, and C, and a faint one D located near the lens galaxy. The redshifts of the source and the lens are $z_S = 3.62$ and $z_L = 0.34$, respectively. In what follows, we assume the following cosmological parameters: $\Omega_m = 0.3$, $\Omega_\Lambda = 0.7$ and $h = 0.7$, giving $D_L = 1.00$ Gpc and $D_S = 1.49$ Gpc.

To model the macro-lensing system, we adopt a singular isothermal ellipsoid (SIE) in an external shear field in which the isopotential curves in the projected surface perpendicular to the line of sight are ellipse (Kormann et al. 1994). This lens model has the following parameters: Einstein angular radius θ_E , a ratio q of the minor axis to the major axis of the ellipse of the iso-potential contour, position angle ϕ_g of the minor axis, source position on the source plane, lens position on the lens plane, unlensed source flux, strength and direction of the external shear (γ, ϕ_s). The best-fit lensing parameters using χ^2 fit is $\theta_E = 0.78$ arcsec, $q = 0.84$, $\phi_g = -57.5^\circ$, $\gamma = 0.21$, $\phi_s = -53.9^\circ$ (Chiba 2002), where the one-dimensional velocity dispersion of the lens is estimated as $\sigma = 183.23 \text{ km s}^{-1}$. The observed position of each image is taken from HST observations with the Faint Object Camera by Impey et al (1996). We show, in the middle panel of Figure 1, the model results for the

four lensed images. It should be noted that B1422+231 shows an anomalous flux ratio in the macro-lensed images possibly caused by the CDM subhalos with masses larger than $10^6 M_\odot$ (Chiba 2002). We neglect below the effects of such subhalos which are not relevant to microlensing by MASCOs.

We estimate the surface number density of MASCOs with an individual mass of M in the lens galaxy. Because the ellipticity of the lens in B1422+231 is modest, it can be approximated by that of a singular isothermal sphere (SIS) with surface mass density $\Sigma(R) = \sigma^2 / 2GR$ where R is the projected radial distance from the lens center. The radial distances of the images A, B, and C from the center are roughly equal to the linear Einstein radius, $\xi_0 \equiv D_L \theta_E = 3.8$ kpc. Note that 1 mas corresponds to ~ 4.9 pc on the lens plane. Then the surface number density of MASCOs at $R = \xi_0$ is estimated as $N(\xi_0) = f \Sigma(\xi_0) / M \sim f \times 2.4 \times 10^2 (M / 10^2 M_\odot)^{-1} \text{ mas}^{-2}$, where $f \leq 1$ is a parameter that represents the fraction of MASCOs in the total mass of the dark halo. For the D image, the surface number density will be 2.7 times larger because the radial distance is as small as $R = \xi_0 / 2.7$. Assuming that the observable radio-emitting region of the QSO has a typical linear size of the order of ~ 10 pc, then the total number of MASCOs overlaid on the macro-lensed images would be several for $M = 10^2 M_\odot$ even if the MASCO fraction is of the order of a few percents. The presence of more extended jets in the images will increase this number.

First, we assume that MASCOs are placed randomly on the lens plane in which the mean number is determined by the surface number density $N(R)$. Clustering of MASCOs on subgalactic scales will not be considered for the sake of simplicity; if a clustering signature is observed in the lensed images, it will give us a valuable information about the formation process of MASCOs.

Second, we calculate the total gravitational potential of the lens from the sum of a SIE that best fits the position and the flux ratios of the four macro-lensed images and perturbers, whereas the consistent calculation should arrange this combined lens potential rather than the potential of the SIE alone. However, this simplification does not affect the concerned microlensing signatures by MASCOs. In our simulation, MASCOs are represented by point masses which perturb the macro-lens. We also carry out similar calculation in which the perturbers are represented by SISs for comparison. We also assume that the unlensed QSO image has a circular symmetry with a radial profile given by the Gaussian distribution with a standard deviation $3h^{-1}$ pc.

3. RESULTS

Four panels in Figure 1 show the portions of four macro images disturbed by the point-mass MASCOs with $M = 10^2 M_\odot$ and $f = 0.06$, where a resolution of 0.01 mas is assumed. One can clearly see several dark spots in the brightest part of the macro images as well as several neighboring pairs of dark and bright spots in the region where the surface brightness of the image has a spatial gradient. These characteristic properties of microlensing by point masses can be explained in the following manner.

Let a point mass be located at $\mathbf{x} = 0$ on the lens plane for the extended image on the source plane with coordinate \mathbf{y} , where both \mathbf{x} and \mathbf{y} are measured in units of the Einstein radius of a MASCO. The lens equation is then given by $\mathbf{y} = \mathbf{x} - \mathbf{x}/x^2$. It follows that the positions on the lens plane within the Einstein

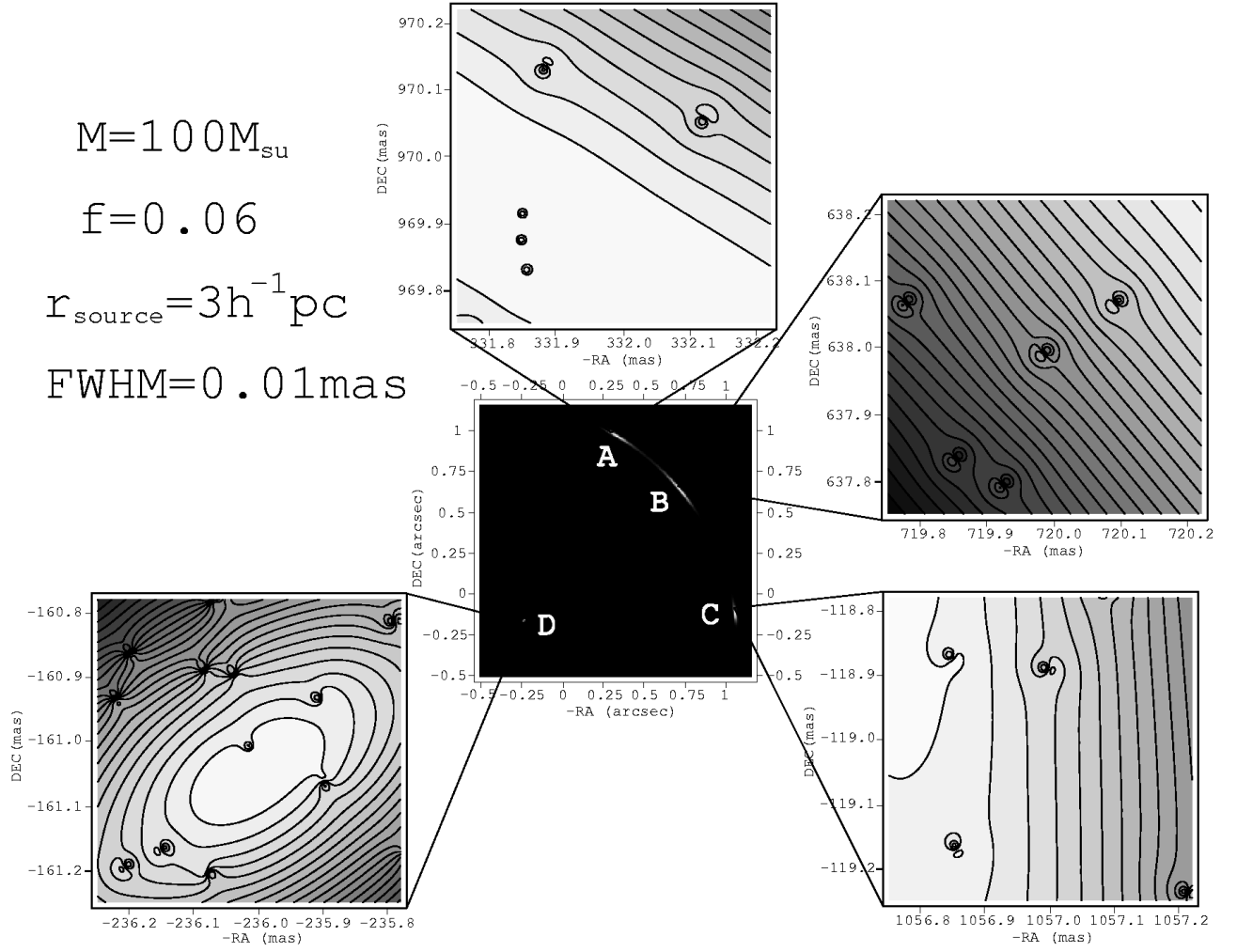


FIG. 1.— A simulation of radio maps of B1422+231 smoothed by a Gaussian beam with $\text{FWHM}=0.01\text{mas}$. MASCOs are represented by point masses with mass $M = 10^2 M_{\odot}$. Dark spots in zoomed four images correspond to MASCOs in the dark halo of the foreground galaxy. The iso-surface brightness contour interval is 1/40 of the maximum value. The MASCO fraction to the dark matter halo is assumed to be $f=0.06$ corresponding to MASCO density $\Omega_* \sim 0.018$ provided that the total matter density is $\Omega_m=0.3$.

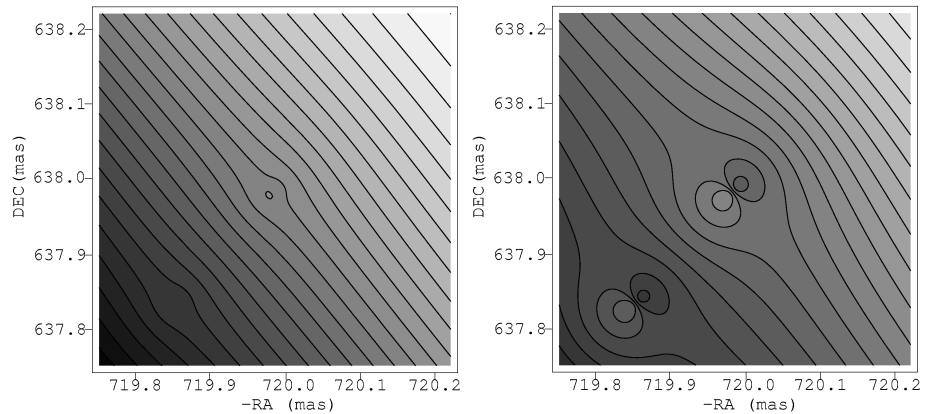


FIG. 2.— Simulations of radio maps of B image in B1422+231 smoothed by a Gaussian beam with $\text{FWHM}=0.01\text{mas}$ in which singular isothermal spheres with mass $M = 10^4 M_{\odot}$ are placed randomly in the dark halo. The ratio of the SIS radius to the tidal disruption radius is 1(left) and 1/4(right).

radius satisfying $-0.62 \lesssim x < 0$ are mapped to $y > 1$. Conversely, the source image extended outside the Einstein radius is mapped to the lens-plane region with radius $x = 0.62$ inside the Einstein radius. Suppose that the surface brightness of the source has a profile $\sigma_y = y^{-\beta}$ with $\beta > 0$. Then, in the neighborhood of the lens center $x = \epsilon \ll 1$ with $\epsilon > 0$, the surface brightness of the lensed image, σ_x , is decreased as $\sigma_x = \epsilon^\beta$. Thus, if σ_y decreases monotonically with increasing distance from the lens center, then one would observe a dark spot (inside the Einstein radius) at the lens center. If the sign of β is minus, then one would observe a bright spot within the Einstein radius. Therefore, there will be a neighboring pair of dark and bright spots (within the Einstein radius) in the region mapped from the source plane where the gradient of σ_y has a non-vanishing constant value. For less massive MASCOs, such discontinuous changes of the lensed image become inconspicuous because the change in the surface brightness on the scale of the Einstein radius becomes smaller. However, if the source has an intrinsic substructure, it may have a locally large gradient in its surface brightness, yielding pairs of dark and bright spots in the lensed image even for less massive MASCOs. It is worth noting that we can easily distinguish these microlensing effects from any intrinsic structures of the source by linearly mapping the macro-lensed image to one of the other images.

Figure 2 shows the microlensing effects of the SISs with $M = 10^4 M_\odot$ on the B image. In this case, the size of each SIS, r_{SIS} , is a free parameter, affecting the strength of the lensing effect. Its upper limit is set by a tidal radius, $r_t = (GMr^2/\pi\sigma^2)^{1/3}$, at its position r from the galaxy center. We examine two cases, $r_{\text{SIS}}/r_t = 1$ and $1/4$, when r is defined as the projected distance of the image B from the galaxy center, i.e., $r = \xi_0$. In the SIS model, the lens equation is given as $\mathbf{y} = \mathbf{x} - \mathbf{x}/x$. In sharp contrast to the point mass model, the source image extended outside the Einstein radius $y > 1$ cannot be mapped to the region inside the Einstein radius $x < 1$, indicating that there will be almost no visible effect from a lens placed in the region where the gradient in the surface brightness within the Einstein radius vanishes. On the other hand, in the region where the surface brightness gradient does not vanish, a discontinuous change of the image brightness on the scale of the Einstein radius is observed, as found for the point-mass model. However, magnification or demagnification effect by SISs is less conspicuous than the point-mass model.

4. SUMMARY AND DISCUSSION

In this *Letter*, we proposed a method to directly detect MASCOs, i.e., massive compact objects with mass $M = 10^{1-4} M_\odot$

in extragalactic dark halos. Using the VLBI techniques, radio maps of strongly lensed radio-loud QSO with extremely high resolution ~ 0.01 mas would reveal the abundance, the spatial distribution, and the mass density profile of the MASCOs.

We present numerical simulations for B1422+231, a typical strongly lensed QSO system. In the presence of MASCOs, tiny dark spots and pairs of dark and bright spots will appear in the macro-lensed images. From the size of the spot, one can estimate the mass of the MASCO. Even if the total mass of MASCOs in the dark halo of the lens galaxy constitutes only a few percents of the total dark halo mass, we can detect MASCOs from characteristic substructures in the map of the lensed QSO image which cannot be linearly mapped to other macro-lensed images. If a perturbing object of the macro-lensed image is described by a SIS, the signature of microlensing appears only if the gradient in the surface brightness is very large or the size of the SIS is sufficiently compact. In contrast to the point-mass case, light from the fringe of the source is not visible within the Einstein radius. Therefore, one can distinguish SISs from point masses by analyzing the detailed spatial variation in the surface brightness.

If the WMAP result of the Thompson optical depth withstands future data, we will have strong observational evidence that the primordial stars are massive and their formation rate is quite large (Cen 2003). For mass ranges of $50 M_\odot \lesssim M \lesssim 100 M_\odot$ and $260 M_\odot \lesssim M$, the progenitor of the primordial gas can directly collapse to form massive black holes without ejecting any metals (Woosley 1986). Thus the primordial star remnants may constitute a large fraction of the baryonic dark matter. Because our proposed method is so powerful in constraining the abundance of point-mass MASCOs, we might be able to constrain or determine the initial mass function of the primordial stars from the observed mass and the abundance of the MASCOs.

If the CDM is strongly clustered on MASCO mass scales, their subhalos might be detected by our proposed method if they are compact enough. In our simulation, with resolution of 0.01 mas, SIS with mass $M \sim 10^4 M_\odot$ can be detected if the ratio of the tidal disruption radius to the SIS cutoff radius is $\lesssim 4$. By numerically estimating the abundance of subhalos on MASCO scales, one can constrain the amplitude of the initial density fluctuations on such small scales from future radio observations.

We thank S. Kamenno for useful comments on the specification of VSOP-2. This work was supported in part by Grant-in-Aid for Scientific Research Fund (No.11367).

REFERENCES

- Abel, T., Bryan, G. L., & Normann, M. L. 2000, *ApJ*, 540, 39
- Alcock, C. et al. 2000, *ApJ*, 542, 281
- Bennett, C. L., et al. 2003, *astro-ph/0302207*
- Bond, J. R., Arnett, W. D., & Carr, B. J. 1984, *ApJ*, 280, 825
- Bromm, V., Coppi, P. S., & Larson, R. B. 1999, *ApJ*, 527, L5
- Carr, B. J. 1975, *ApJ*, 201, 1
- Cen, R. 2003, *astro-ph/0303236*
- Chiba, M. 2002, *ApJ*, 565, 17
- Gould, G. 1992, *ApJ*, 392, 442
- Hirabayashi, H. et al. 2001, in *ASP Conf. Ser. 251, New Century of X-ray Astronomy*, eds. H. Inoue, & H. Kunieda, (San Francisco: ASP), 540
- Impey, C. D., Foltz, C. B., Petry, C. E., Browne, I. W. A., & Patnaik, A. R. 1996, *ApJ*, 462, L53
- Kormann, R., Schneider, P., & Bartelmann, M. 1994, *A&A*, 284, 285
- Nemiroff, R. J. 1991, *Phys. Rev. Lett.*, 86, 580
- Omukai, K. & Palla, F. 2002, *Ap&SS*, 281, 71
- Schneider, R., Ferrara, A., Natarajan, P. & Omkai, K. 2002, *ApJ*, 571, 30
- Totani, T. 2003, *ApJ*, 586, 735
- Tsuribe, T. & Inutsuka, S. 2001 *Ap&SS*, 276, 1097
- Wambsganss, J. & Paczyński, B. 1992, *ApJ*, 397, L1
- Woosley, S. E. 1986, *ApJ*, 307, 675